Published online: March 13, 2007

Molecular Systems Biology 3; Article number 91; doi:10.1038/msb4100135
Citation: ***Molecular Systems Biology*** **3:91**

www.molecularsystemsbiology.com

molecular systems biology

Gyrase inhibitors induce an oxidative damage cellular death pathway in *Escherichia coli*

Daniel J Dwyer[1,2,6], Michael A Kohanski[2,3,4,6], Boris Hayete[2,5] and James J Collins[1,2,3,5,*]

[1] Program in Molecular Biology, Cell Biology and Biochemistry, Boston University, Boston, MA, USA, [2] Center for BioDynamics and Center for Advanced Biotechnology, Boston University, Boston, MA, USA, [3] Department of Biomedical Engineering, Boston University, Boston, MA, USA, [4] Boston University School of Medicine, Boston, MA, USA and [5] Bioinformatics Program, Boston University, Boston, MA, USA
[6] These authors contributed equally to this work
* Corresponding author. Center for BioDynamics and Department of Biomedical Engineering, Boston University, 44 Cummington Street, Boston, MA 02215, USA. Tel.: +617 353 0390; Fax: +617 353 5462; E-mail: jcollins@bu.edu

Received 10.11.06; accepted 26.1.07

Modulation of bacterial chromosomal supercoiling is a function of DNA gyrase-catalyzed strand breakage and rejoining. This reaction is exploited by both antibiotic and proteic gyrase inhibitors, which trap the gyrase molecule at the DNA cleavage stage. Owing to this interaction, double-stranded DNA breaks are introduced and replication machinery is arrested at blocked replication forks. This immediately results in bacteriostasis and ultimately induces cell death. Here we demonstrate, through a series of phenotypic and gene expression analyses, that superoxide and hydroxyl radical oxidative species are generated following gyrase poisoning and play an important role in cell killing by gyrase inhibitors. We show that superoxide-mediated oxidation of iron–sulfur clusters promotes a breakdown of iron regulatory dynamics; in turn, iron misregulation drives the generation of highly destructive hydroxyl radicals via the Fenton reaction. Importantly, our data reveal that blockage of hydroxyl radical formation increases the survival of gyrase-poisoned cells. Together, this series of biochemical reactions appears to compose a maladaptive response, that serves to amplify the primary effect of gyrase inhibition by oxidatively damaging DNA, proteins and lipids.
Molecular Systems Biology 13 March 2007; doi:10.1038/msb4100135
Subject Categories: cellular metabolism; microbiology & pathogenesis
Keywords: gyrase inhibitors; hydroxyl radicals; iron–sulfur cluster; oxidative damage; systems biology

Introduction

Bacterial chromosomal topology is maintained by the activities of topoisomerase I, topoisomerase IV and DNA gyrase (topoisomerase II) (Champoux, 2001). The gyrase enzyme is responsible for the introduction of negative DNA supercoils in an ATP-dependent manner, and participates in the processes of replication, transcription, repair, recombination and decatenation (Gellert *et al*, 1976; Cozzarelli, 1980; Wang, 1996). Gyrase is composed of two subunits, *gyrA* and *gyrB*, and complexes with its DNA substrate as an A_2B_2 tetramer (Mizuuchi *et al*, 1978; Sugino *et al*, 1980). GyrA catalyzes the concomitant double-stranded breakage and rejoining of DNA phosphodiester bonds following binding and hydrolysis of ATP by GyrB (Gellert, 1981; Reece and Maxwell, 1991).

The interaction between gyrase inhibitors and the GyrA subunit converts DNA gyrase into a lesion-inducing agent, which results in widespread generation of double-stranded DNA breaks (Maki *et al*, 1992; Bernard *et al*, 1993; Chen *et al*, 1996). DNA damage formation rapidly induces cell division arrest, initially driving entry into bacteriostasis (Hanawalt, 1966; Jaffe *et al*, 1985; Drlica and Zhao, 1997). In time, the stable DNA–GyrA–inhibitor complex sterically inhibits replication and transcription by establishing a roadblock to DNA and RNA polymerases, respectively, at stalled replication forks (Kreuzer and Cozzarelli, 1979; Bernard and Couturier, 1992; Willmott *et al*, 1994; Cox *et al*, 2000). This deadly barrier impedes lesion repair while preventing new DNA synthesis, eventually killing the bacterium (Critchlow *et al*, 1997; Drlica and Zhao, 1997; Couturier *et al*, 1998).

In this work, we performed phenotypic, genetic and microarray analyses on gyrase-inhibited *Escherichia coli* to identify additional contributors to cell death resulting from gyrase poisoning. Taking a systems biology approach, we enriched our gene expression data using transcription factor and functional pathway classifications. This analysis expectedly revealed that the expression of DNA damage response and repair genes was markedly upregulated following inhibition of DNA gyrase and the generation of DNA lesions. Surprisingly, however, we also observed significantly upregulated expression of genes related to superoxide stress, iron–sulfur (Fe–S) cluster synthesis and iron uptake and utilization.

The unfortunate byproduct of increased aerobic respiratory activity and oxidative phosphorylation is the increased formation of the reactive oxygen species (ROS), superoxide (Imlay and Fridovich, 1991). Although superoxide itself presents no additional direct threat to DNA, cytosolic dehydratase proteins containing Fe–S clusters are highly susceptible to oxidative

attack (Liochev and Fridovich, 1999; Imlay, 2003, 2006). Various methods have been used to show that superoxide-mediated decomposition of Fe–S clusters, following shifts between anaerobic and aerobic growth states, leads to cytoplasmic release of ferrous (II) iron (Keyer and Imlay, 1996; Liochev, 1996). Elevated intracellular concentrations of ferrous iron have been shown to mediate DNA damage either directly (Henle *et al*, 1999; Rai *et al*, 2001) or via the formation of additional oxidative molecules (Touati, 2000; Imlay, 2003). Hydroxyl radicals, a highly destructive ROS, are the product of the Fenton reaction (Imlay *et al*, 1988; Imlay and Linn, 1988), in which ferrous iron mediates the reduction of hydrogen peroxide. These biologically threatening oxidative species are capable of inducing a wide array of mutagenic single-base substitutions and DNA adducts (Aruoma *et al*, 1989; McBride *et al*, 1991; Balasubramanian *et al*, 1998; Nunoshiba *et al*, 1999), as well as damaging peptides and lipids (Farr and Kogoma, 1991).

Interestingly, the generation of hydroxyl radicals following DNA damage has been shown in higher order systems, including mammalian cells, and is considered as one of the hallmark features of apoptosis (Jacobson, 1996; Simon *et al*, 2000). Here, we provide direct evidence that hydroxyl radicals are generated in bacteria following both antibiotic- and peptide-based gyrase poisoning. Our results show that hydroxyl radical production, upon gyrase inhibition, is directly related to the presence and status of Fe–S cluster-containing proteins. In turn, our data suggest that cycling of Fe–S clusters between oxidized and reduced states contributes to a breakdown in endogenous iron regulatory dynamics and global iron management. We thus propose that ROS contribute significantly to bacterial cell death following gyrase inhibition and that the associated series of biochemical reactions represents a maladaptive response to aerobic growth which promotes terminal cell fate.

Results

Phenotypic response to DNA gyrase inhibition

We initially sought to characterize the *in vivo* response of the wild-type *E. coli* strain BW25113 (Wanner, 1983) to gyrase inhibition and to identify additional contributors to cell death following gyrase poisoning. To accomplish this, we employed the synthetic quinolone antibiotic, norfloxacin, and the natural peptide toxin, CcdB (a component of the F plasmid-encoded CcdB–CcdA toxin–antitoxin system; Miki *et al*, 1992). Upon treatment with norfloxacin, we observed an immediate 2-log reduction in colony forming units (CFU/ml) (Figure 1A). These values steadily declined for the remainder of our experiments. Induction of CcdB expression similarly resulted in consistent CFU/ml reduction over the first 3 h of our experiments (Figure 1A). Wild-type cells expressing CcdB, however, routinely reached their minimum density at the 3 h time point, and then began a sustained increase in cell density that continued over the remainder of the experiment.

Although these results show that, in our system, CcdB is not as efficient as norfloxacin in its ability to induce cellular death in BW25113 cells, our data suggested that both gyrase inhibitors rapidly induce DNA lesion formation. To confirm this hypothesis, we employed an engineered, DNA damage-inducible reporter gene construct that relies upon LexA repression for tight regulation of *gfp* transcription; fluorescence output is thus reflective of RecA-stimulated autocleavage of LexA following DNA damage recognition (Little, 1991). As anticipated, gyrase poisoning of wild-type bacteria resulted in significant GFP expression from this construct (Figures 1B and C). Norfloxacin treatment uniformly induced high levels of fluorescence (Figure 1B), demonstrating the efficiency and highlighting the irreversibility with which the quinolone traps gyrase and stimulates the formation of DNA breaks. We also observed a large shift in fluorescence upon expression of CcdB, indicative of widespread DNA damage (Figure 1C). In line with our CcdB+ growth data (and the relative inefficiency of CcdB-mediated cell killing compared with norfloxacin in our system), the broad DNA damage-related fluorescence distribution exhibited by CcdB+ cells suggests that DNA damage is being corrected by endogenous repair systems. Taken together, these phenotypic data confirm that norfloxacin and CcdB are both potent inhibitors of DNA gyrase that promote the rapid generation of DNA lesions.

Gene expression response to DNA gyrase inhibition

We next examined the transcriptional response of wild-type *E. coli* cells treated with norfloxacin or expressing CcdB, with the goal of identifying potential secondary contributors to cell death. Analysis of our time-course microarray data revealed that >800 genes exhibited statistically significant upregulation or downregulation at one or more time points as a function of each respective inhibitor (Supplementary Table 1); significance (*z*-score) was determined on a gene by gene basis, by comparison of mean expression levels to a large (~500) compendium of *E. coli* microarray data collected under a wide array of conditions (see Materials and methods and Supplementary information for details).

Taking a systems biology approach, we first applied gene ontology (GO) (Ashburner *et al*, 2000; Camon *et al*, 2004) classifications to categorize this gene list by biological function, and then enriched these data using GO::TermFinder (Boyle *et al*, 2004), which enabled us to determine the significance of these classifications (Supplementary Figures 1 and 2; Supplementary Table 2). We next employed the RegulonDB database (Salgado *et al*, 2006) of known transcription factor connections, in conjunction with a published map of transcriptional regulation (Faith *et al*, 2007), to focus on transcription factors whose targets were significantly enriched in our data set (Supplementary Table 3). These measures thus allowed us to group genes based on regulatory and functional pathway classifications and to identify coordinated responses to gyrase inhibition.

As expected, LexA, which coordinates the expression of the SOS DNA damage response program, was found to be among the most overrepresented transcriptional regulators following norfloxacin treatment and CcdB expression; this result served to further validate our growth data and DNA damage reporter results. As highlighted in Figure 2, DNA damage-inducible genes comprised one of the largest and most strongly

Published online: March 13, 2007

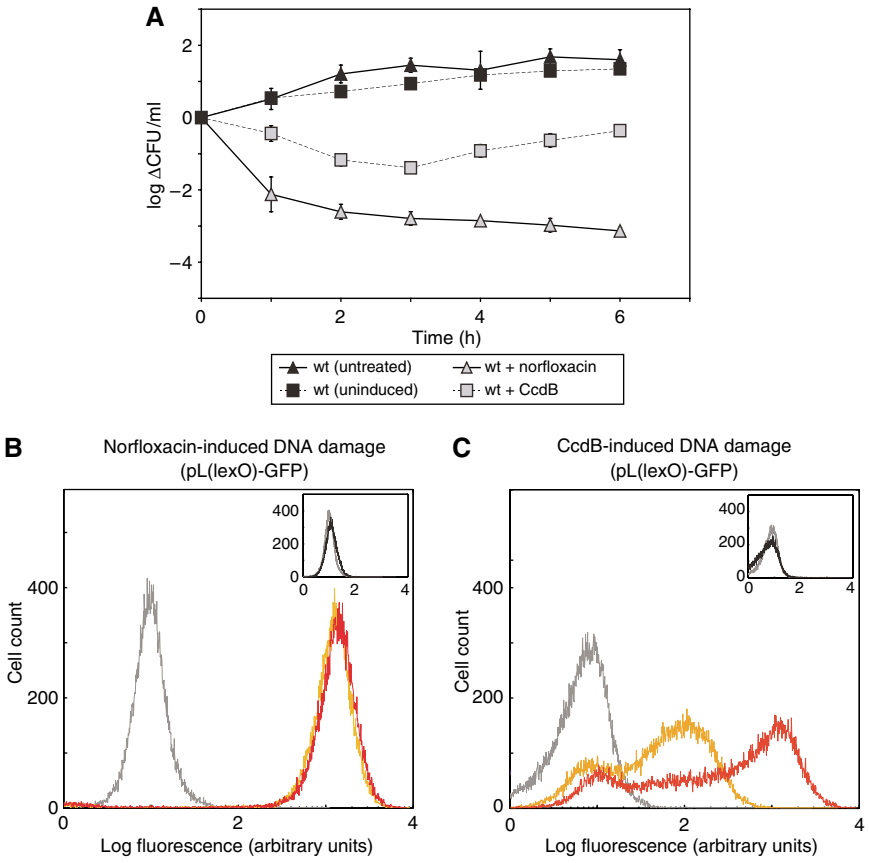

Figure 1 Phenotypic response to gyrase inhibition. (**A**) Log change in colony forming units per ml (CFU/ml) of wild-type, BW25113 *E. coli* cells (mean ± s.d.). Untreated (black triangles, solid line) and uninduced (harboring CcdB plasmid; black squares, dashed line) cell growth, respectively, was compared with the growth of norfloxacin-treated (250 ng/ml; gray triangles, solid line) and CcdB-expressing (gray squares, dashed line) cultures. (**B, C**) Induction of DNA damage by gyrase inhibitors. To confirm the occurrence of DNA damage following gyrase poisoning, we employed an engineered promoter-GFP reporter gene construct, pL(lexO)-GFP. LexA cleavage, and thus DNA lesion formation, could be examined at single-cell resolution by measuring green fluorescent protein expression using a flow cytometer. Shown are representative fluorescence population distributions of wild-type cultures (B) treated with norfloxacin, or (C) expressing CcdB, before (time zero, gray) and after (3 h (orange) and 6 h (red)) gyrase inhibition. The respective insets show representative control fluorescence measurements of uninhibited wild-type cultures at time zero (gray) and 6 h (black).

perturbed functional groups in our study. This again is consistent with activation of both the SOS response pathway and the Din (damage-inducible) family of genes (Witkin, 1976; McEntee, 1977; Kenyon and Walker, 1980; Little and Mount, 1982; Walker, 1984; Courcelle and Hanawalt, 2003; Friedberg *et al*, 2005). The strongest responding among these repair-related genes were error-prone DNA polymerases IV (DinP) and V (composed of UmuC and UmuD) (Elledge and Walker, 1983; Sutton and Walker, 2001).

Interestingly, we also observed statistically significant enrichment for the IscR (iron–sulfur cluster regulator) transcription factor as a function of each perturbation. IscR has been shown to autoregulate expression of the *iscRUSA* operon of genes, which are primarily involved in *de novo* Fe–S cluster assembly. The repair of heavily oxidized Fe–S clusters is believed to require the activity of the Isc protein family, and the derepression of the *iscRUSA* operon following oxidant stress has been previously explored (Schwartz *et al*, 2000; Djaman *et al*, 2004).

Along these lines, additional analysis of our microarray results revealed that the oxidative stress response regulator SoxS was also significantly enriched in our data set. Treatment of *E. coli* with either norfloxacin or CcdB induced the superoxide response operon, *soxRS* (Figure 2). Transcription of *soxS* is positively regulated by SoxR and is stimulated upon SoxR activation, the result of superoxide-induced (yet reversible) oxidation of SoxR's Fe–S cluster (Gaudu *et al*, 1997; Hidalgo *et al*, 1998). The SoxS transcription factor is known to activate expression of the manganese-superoxide dismutase, *sodA*, considered as the first responder in the protection of biomolecules from superoxide-induced damage (Hopkin *et al*, 1992). SodA, like SoxS, was among our list of significantly upregulated genes following norfloxacin treatment or CcdB expression (Figure 2). That damage to Fe–S clusters was occurring as a function of gyrase poisoning was further supported by the observation that each component of the *iscRSUA* operon exhibited highly increased expression upon inhibition of gyrase (Figure 2).

SoxS has also been shown to activate expression of *fur*, a ferrous (II) iron-binding transcription factor that regulates the expression of iron uptake, utilization and homeostasis genes (Escolar *et al*, 1999; Andrews *et al*, 2003). As highlighted in

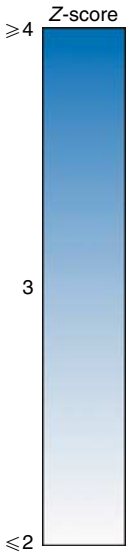

DNA damage response		
Norfloxacin		CcdB
4.6	DinD	4.3
<2.0	DinF	3.4
3.8	DinG	2.1
4.3	DinI	4.9
4.6	DinP	3.0
2.1	LexA	3.1
4.0	OraA	3.7
3.9	PolB	<2.0
3.0	RecA	3.2
4.1	RecN	4.2
3.1	RuvA	3.9
2.7	RuvB	2.8
2.4	SbmC	<2.0
<2.0	Ssb	2.4
4.3	SulA	4.0
5.9	UmuC	5.3
5.4	UmuD	4.8
<2.0	UvrA	2.1
2.3	UvrB	<2.0
2.7	UvrD	3.6

Iron uptake and utilization		
Norfloxacin		CcdB
2.6	EntC	<2.0
2.1	ExbB	2.5
2.5	ExbD	2.7
2.1	FecI	2.5
2.1	FecR	<2.0
3.1	FepB	<2.0
2.2	FepC	<2.0
2.5	Fes	<2.0
2.0	FhuA	2.0
<2.0	FhuB	2.6
2.1	FhuC	2.6
3.1	FhuF	3.0
2.3	NrdH	<2.0
2.2	NrdI	<2.0
3.0	SodA	3.2
<2.0	TonB	2.3

Oxidative damage response		
Norfloxacin		CcdB
<2.0	MarA	3.2
2.0	MarB	3.0
<2.0	MarR	3.1
3.0	SodA	3.2
2.8	SoxS	4.5

Iron–sulfur cluster synthesis		
Norfloxacin		CcdB
2.2	IscA	3.4
2.8	IscR	2.6
2.9	IscS	3.4
2.5	IscU	3.2

Figure 2 Transcriptome response to gyrase inhibition. Highlighted is a portion of the functionally enriched gene expression response of norfloxacin-treated or CcdB-expressing wild-type cells. Relative weighted *z*-scores (a measure of standard deviation) were calculated for each gene, based on comparison to mean expression values derived from a large (~500) database of microarray data; these values were then normalized by subtracting the corresponding uninduced sample *z*-scores. Using biochemical pathway and transcription factor regulatory classifications, we identified significantly upregulated functional units that responded in a coordinated manner. For each functional unit, genes that exhibited a weighted *z*-score ⩾2 standard deviations are shown; scale is shown on left. This analysis is described in greater detail in Materials and methods and Supplementary information. Additionally, all gyrase inhibitor microarray results can be found in Supplementary information.

Figure 2, a number of Fur-regulated iron uptake-related genes were among those genes found to be significantly upregulated by norfloxacin or CcdB. Specifically, we observed increased expression of siderophore-based iron acquisition systems, including components of the Fe^{3+}-siderophore receptor/permease Fec, Fep and Fhu families, as well as the energy transducing TonB–ExbBD complex, which provides the energy required for active siderophore transport.

Gyrase inhibition induces hydroxyl radical formation

In the Fenton reaction, free ferrous iron reacts with hydrogen peroxide to generate highly destructive hydroxyl radicals (Imlay, 2003). Superoxide, via oxidative damage to Fe–S clusters and iron leaching, has been shown to play a critical role in the generation of hydroxyl radicals. Based on our microarray results and previous studies, we hypothesized that production of hydroxyl radicals may be the cytotoxic end product of a surge in superoxide and Fe–S cluster cycling following gyrase inhibition. To detect the generation of hydroxyl radicals upon gyrase poisoning by norfloxacin or CcdB, we employed the fluorescent reporter dye, 3′-(*p*-hydroxyphenyl) fluorescein (HPF) (Setsukinai *et al*, 2003), which is oxidized by hydroxyl radicals with high specificity.

We detected a significant increase in hydroxyl radical-induced HPF fluorescence at both 3 and 6 h post-treatment of wild-type *E. coli* with norfloxacin (Figure 3A). Similarly, expression of CcdB in wild-type *E. coli* also resulted in a large HPF fluorescence increase at both 3 and 6 h post-induction (Figure 3B). Importantly, untreated cultures did not show any detectable increase in HPF fluorescence for the duration of our experiments. These data show that inhibition of DNA gyrase and the generation of double-stranded DNA breaks lead to environmental changes that promote the formation of deleterious hydroxyl radicals.

To demonstrate that generation of hydroxyl radicals was related to the Fenton reaction and an available pool of reactive iron, we repeated our HPF fluorescence measurements in the presence of the iron chelator, *o*-phenanthroline. This chelator has been previously used to block the effects of the Fenton reaction in bacteria exposed to hydrogen peroxide (Imlay *et al*, 1988; Asad and Leitao, 1991) and to uncover the role of free radical damage in mitochondria (Yang *et al*, 1958; de Mello Filho and Meneghini, 1985). As anticipated, *o*-phenanthroline inhibited the formation of hydroxyl radicals following gyrase

Published online: March 13, 2007

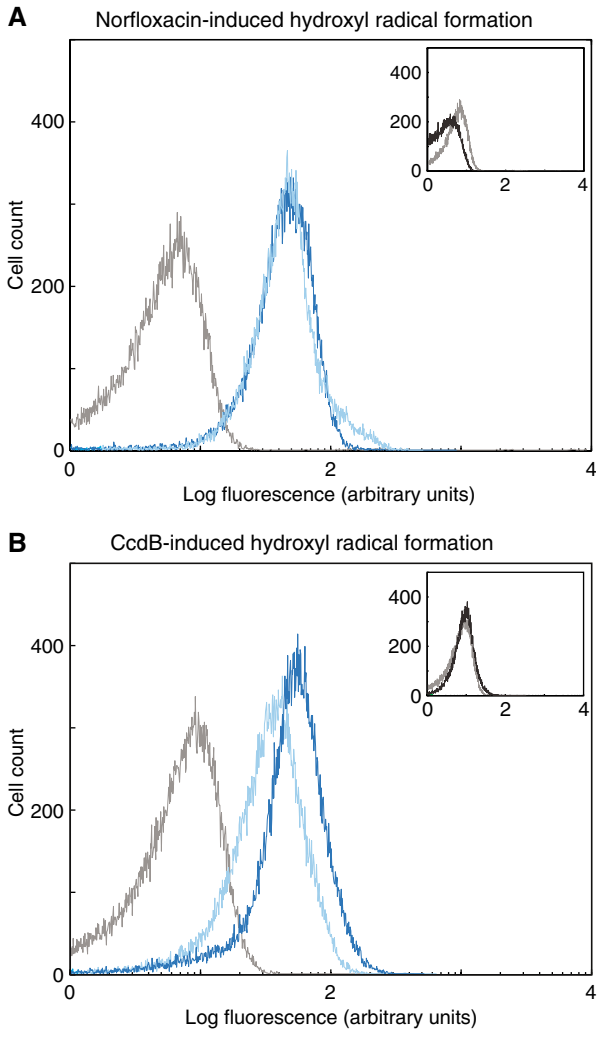

Figure 3 Generation of hydroxyl radicals following gyrase inhibition. Formation of oxidatively damaging hydroxyl radicals was measured using the highly specific fluorescent dye, HPF. Hydroxyl radical generation was observed following both (**A**) norfloxacin treatment and (**B**) CcdB expression. Representative flow cytometer-measured fluorescence population distributions of wild-type cells before (time zero, gray) and after (3 h (light blue) and 6 h (blue)) gyrase inhibition are shown. The respective insets show representative control fluorescence population distributions of uninhibited wild-type cultures at time zero (gray) and 6 h (black).

inhibition by norfloxacin (Figure 4A) or CcdB (Figure 4B) for the duration of the respective experiments.

To determine the effect of hydroxyl radical-induced oxidative damage on the survival of gyrase-inhibited *E. coli*, we performed growth studies in the presence of Fenton reaction-neutralizing *o*-phenanthroline. Addition of the chelator to cultures treated with norfloxacin significantly inhibited cell killing, essentially rendering the drug bacteriostatic (Figure 4C). While the attenuation of cell death in CcdB-expressing cells was not as dramatic, we did observe a greater than 0.5-log increase in CFU/ml before recovery around 2 h (Figure 4C). Our findings thus provide strong evidence for the involvement of hydroxyl radicals in gyrase inhibitor-induced cell death.

Finally, to show that the observed generation of hydroxyl radicals following norfloxacin application was not related to direct redox cycling of the antibiotic, we examined hydroxyl radical formation and survival in two *gyrA* mutant *E. coli* strains; these strains, RFS289 (*gyrA111*) (Schleif, 1972) and KL317 (*gyrA17*) (Norkin, 1970), are both known to be resistant to the quinolone, nalidixic acid. Treatment with norfloxacin of both mutant strains did not result in loss of cellular viability, proving that these specific *gyrA* mutations likewise confer resistance to norfloxacin (Supplementary Figure 3). More importantly, we did not observe an increase in hydroxyl radical formation following norfloxacin treatment of these strains (Supplementary Figure 3). These results clearly show that norfloxacin-mediated hydroxyl radical formation occurs only when cell death is observed and as a consequence of the interaction between gyrase and the gyrase inhibitor.

Iron misregulation following gyrase inhibition

As our hydroxyl radical-sensitive dye experiments revealed, Fenton-reactive iron plays a critical role in cell killing by gyrase inhibitors. To explore whether this hydroxyl radical-generating iron was derived exogenously (Fur-related uptake), endogenously (Fe–S clusters) or from both sources, we first performed growth studies on a series of iron-related single-gene knockouts. To more rapidly perform genetic screening of knockout strains, we initially employed norfloxacin in our phenotypic analyses; the CcdB results are presented in Supplementary information.

Previous work has shown that a deletion of the iron regulator, Fur, leads to an intracellular spike in the concentration of 'free iron' and potentiates oxidative damage to *E. coli* DNA (in a Δ*recA* background) (Touati *et al*, 1995). Somewhat surprisingly, we found that a *fur* deletion mutant responded much slower to gyrase inhibition and exhibited enhanced survival compared with wild-type cultures challenged with norfloxacin over the first 3 h of our experiments (Figure 5A). At our final time point, Δ*fur* cultures exhibited a 1-log increase in cellular survival when compared with the wild-type results (an overall 2-log decrease from time zero). Interestingly, ectopic overexpression of Fur from an isopropyl-β-D-thiogalactopyranoside (IPTG)-inducible 'rescue' plasmid, in Δ*fur* cultures treated with norfloxacin, served to restore the rapid reduction in viability observed for gyrase-poisoned wild-type cultures (Supplementary Figure 4).

To further explore the role of Fur in the secondary response to gyrase inhibition, and to determine if DNA and oxidative damage promote derepression of iron uptake and utilization genes, we constructed an iron regulation reporter construct that employs the transcription factor Fur as the mediator of *gfp* expression. Similar in design to our DNA damage reporter construct, fluorescence output from our iron regulatory construct reflects derepression by Fur of an engineered promoter containing Fur operator sites. Following norfloxacin treatment, we observed a large, uniform increase in fluorescence from our Fur-regulated reporter construct, suggesting that gyrase inhibition promotes a breakdown in iron regulatory dynamics (Figure 5B); specifically, norfloxacin induced a 10-fold change, whereas the iron chelator, *o*-phenanthroline, induced a 100-fold change in fluorescence when compared

Published online: March 13, 2007

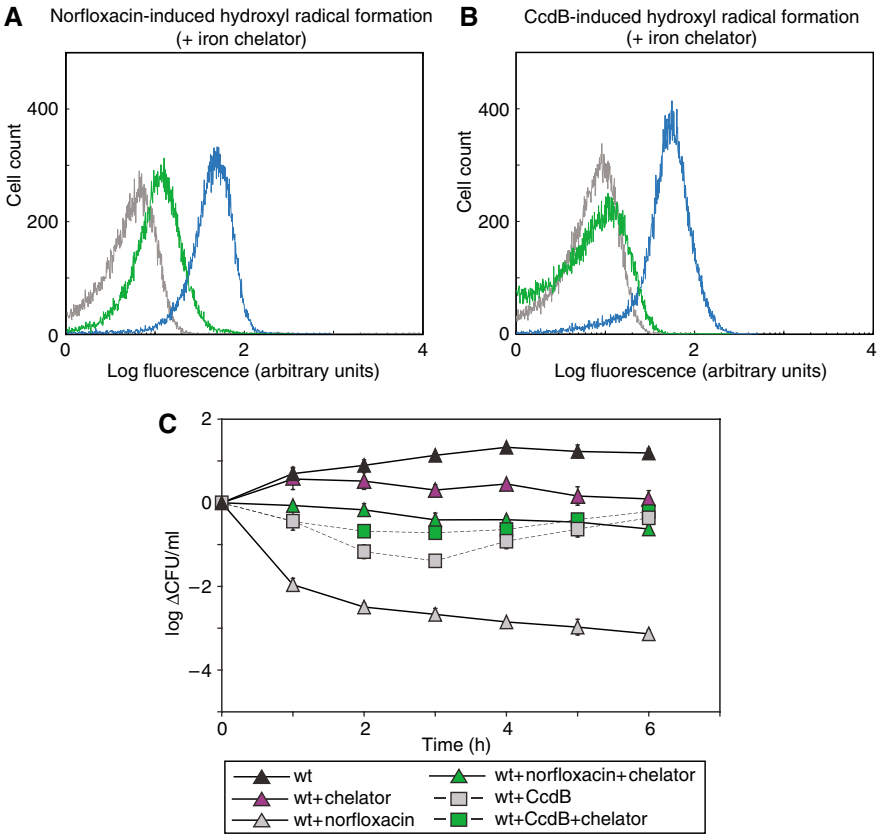

Figure 4 Iron chelation prevents hydroxyl radical formation and reduces gyrase inhibitor-mediated cell death. Application of the iron chelator, *o*-phenanthroline, suppresses the formation of hydroxyl radicals and reduces cell death following gyrase inhibition in wild-type *E. coli* cells. (**A, B**) Using the fluorescent reporter dye, HPF, we monitored the effect of *o*-phenanthroline addition on hydroxyl radical formation in (A) norfloxacin-treated and (B) CcdB-expressing wild-type cells. Representative flow cytometer-measured fluorescence population distributions of wild-type cells before (time zero, gray) and after (6 h (green)) gyrase inhibition, in the presence of the iron chelator are shown. For direct comparison, fluorescent population distributions of gyrase-inhibited cells, at 6 h, in the absence of chelator, are also shown (blue). (**C**) Log change in colony forming units per ml (CFU/ml) of wild-type cells (mean ± s.d.). Cells were grown in the presence of *o*-phenanthroline and treated with norfloxacin (250 ng/ml, green triangles, solid line) or induced to express CcdB (green squares, dashed line). These results were compared with the growth of cells treated with norfloxacin (gray triangles, solid line) or expressing CcdB (gray squares, dashed line) alone. As controls, normal growth (black triangles, solid line) and growth in the presence of *o*-phenanthroline alone (purple triangles, solid line) are shown.

with untreated fluorescence measurements (Supplementary Figure 5). Importantly, we also observed increased expression of GFP from our Fur-regulated reporter construct following CcdB expression (Supplementary Figure 6). This result supports our microarray analysis, which identified Fur-regulated genes as being among the most significantly upregulated as a function of gyrase poisoning.

To determine if impairment of exogenous iron uptake affects the ability of *E. coli* to survive gyrase inhibition, we next examined the phenotypic effect of norfloxacin on a deletion mutant of the import complex gene, *tonB*. Again, the TonB–ExbBD complex controls active iron transport across the inner membrane, in an energy-dependent process, for siderophore uptake systems (Clarke *et al*, 2001). The Δ*tonB* knockout had a negligible effect on the viability of norfloxacin-treated *E. coli* (Figure 5A) compared with our wild-type results (Figure 1A), suggesting that the major iron import system does not play a significant role in gyrase inhibitor-induced cell death. Relative to previous findings, in which exogenous iron import has been implicated in oxidative damage-mediated cell killing (Touati *et al*, 1995), our results imply that an internal disruption of iron management is a critical factor in gyrase inhibitor-mediated cell death.

To test whether this endogenous iron misregulation was related to Fe–S cluster status, we phenotypically examined single-gene knockouts of the Fe–S cluster synthesis operon, *iscRSUA*. Although Δ*iscR*, Δ*iscU* and Δ*iscA* deletion mutants showed slower response to application of norfloxacin, survival levels of these cultures were similar to those of our wild-type cultures within 3 h post-treatment (Supplementary Figure 7). Interestingly, deletion of the cysteine desulfurase, *iscS*, which is critical for efficient Fe–S cluster turnover and plays a role in tRNA modification and thiamine biosynthesis (Schwartz *et al*, 2000; Djaman *et al*, 2004), had the most dramatic effect on survival (Figure 5A). Knocking out this protein, which provides atomic sulfur during Fe–S cluster assembly (Zheng *et al*, 1998), resulted in a near 2-log increase in viability for the majority of the experiment relative to norfloxacin-treated wild-type cultures. Δ*iscS* cultures had a remarkably slow phenotypic response to gyrase inhibition, exhibiting less than 1-log of cell death within the first 4 h post-treatment. We also screened the effect of norfloxacin-based gyrase inhibition on a

Published online: March 13, 2007

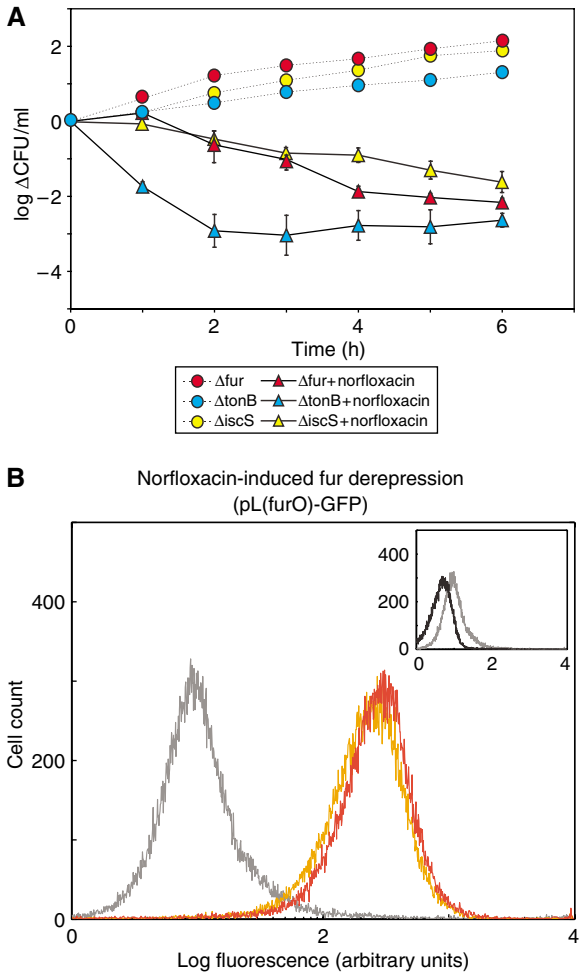

Figure 5 Gyrase inhibition induces iron misregulation. (**A**) Log change in colony forming units per ml (CFU/ml) of BW25113 *E. coli* single-gene deletion strains. Growth curves for untreated deletion strains are shown for comparison purposes and are representative of growth in the absence of perturbation. Survival data for treated samples are represented as mean ± s.d. Survival of Δ*fur* cultures (untreated, red circles, dotted line; norfloxacin-treated, red triangles, solid line), Δ*tonB* cultures (untreated, light blue circles, dotted line; norfloxacin-treated, light blue triangles, solid line) and Δ*iscS* cultures (untreated, yellow circles, dotted line; norfloxacin-treated, yellow triangles, solid line) are shown. (**B**) Misregulation of iron-related genes following gyrase inhibition. To confirm that derepression, by Fur, of iron uptake and utilization genes ocurs upon inhibition of gyrase, we employed an engineered promoter-GFP reporter gene construct, pL(furO)-GFP, and performed flow cytometer-based measurements at single-cell resolution. Representative fluorescence population distributions of norfloxacin-treated wild-type cultures before (time zero, gray) and after (3 h (orange) and 6 h (red)) gyrase inhibition are shown. The respective insets show representative control fluorescence measurements of uninhibited wild-type cultures at time zero (gray) and 6 h (black).

deletion mutant of the *iscS* paralogue, *sufS*. SufS is a component of the *sufABCDSE* operon, which is thought to handle Fe–S cluster assembly not catalyzed by *isc* operon activity during normal growth and is considered to be required for Fe–S cluster assembly in iron-limiting and oxidatively stressful conditions (Djaman *et al*, 2004; Outten *et al*, 2004). We found that the Δ*sufS* knockout had little effect on norfloxacin-mediated cell death and exhibited wild-type levels of survival (Supplementary Figure 7).

It is worth mentioning that Δ*iscS* cultures grew at a slower rate when compared with wild-type cultures in our study, consistent with previous work (Schwartz *et al*, 2000; Djaman *et al*, 2004). However, it is also important to note that the growth rate of Δ*iscS* was similar to Δ*recA* cultures, which showed a near 5-log decrease in viability following norfloxacin application (Supplementary Figure 7). Together, these data suggest that the decreased cell death exhibited by norfloxacin-treated Δ*iscS* cultures is not simply related to drug killing efficiency and rate of growth.

In order to more directly monitor the overall status of Fe–S clusters following gyrase inhibition, we constructed an *iscRUSA* promoter-*gfp* reporter gene fusion construct using the native (−150 to +26) *iscRUSA* operon promoter region (Giel *et al*, 2006). This promoter is negatively regulated by the IscR transcription factor and responds to conditions that are rate limiting for Fe–S cluster biogenesis by upregulating expression of the Isc protein family, including IscR itself (Schwartz *et al*, 2001). Norfloxacin treatment of wild-type cells led to a near five-fold increase in fluorescence at 3 h and more than a 10-fold increase in fluorescence at 6 h when compared with untreated cultures (Figure 6B); CcdB expression also yielded increased fluorescence from our IscR-regulated reporter construct (Supplementary Figure 8).

Oxidative attack of iron–sulfur clusters

In light of our Isc-related results, we next sought to determine whether superoxide-based oxidative attack to Fe–S clusters was indeed occurring by monitoring the activation of the superoxide response. To do so, we constructed a *soxS* promoter-*gfp* reporter gene fusion using the native *soxS* promoter region. This promoter is transcriptionally regulated by SoxR, and its activation is directly related to the redox state of SoxR (superoxide-related oxidation activates transcription; Hidalgo *et al*, 1998). As expected, gyrase inhibition by norfloxacin resulted in GFP expression from this superoxide response sensor (Figure 6A); more specifically, both norfloxacin and the superoxide-generating compound, paraquat (at a concentration of 10 μM; Supplementary Figure 5), induced a 10-fold increase in fluorescence when compared with untreated cultures. We also observed increased fluorescence from our SoxR-regulated reporter construct following CcdB expression (Supplementary Figure 6). Importantly, our baseline (time zero) and untreated control measurements (at 6 h) were remarkably similar (Figure 6A). These data support the phenotypic- and microarray-based hypothesis that oxidation of Fe–S clusters by superoxide is occurring and that the SoxRS response is activated.

We next studied the phenotypic effect of impaired recognition and mitigation of superoxide formation following gyrase inhibition. Whereas expression of the superoxide-sensitive transcription factor SoxS is significantly upregulated upon gyrase inhibition, treatment of a *soxS* deletion mutant with norfloxacin resulted in no discernable difference in survival compared with our wild-type growth data (Supplementary Figure 7). Moreover, we observed no change in the level of cell death when Δ*sodA* (manganese-superoxide dismutase) cultures were challenged with norfloxacin (Supplementary Figure 7).

Published online: March 13, 2007

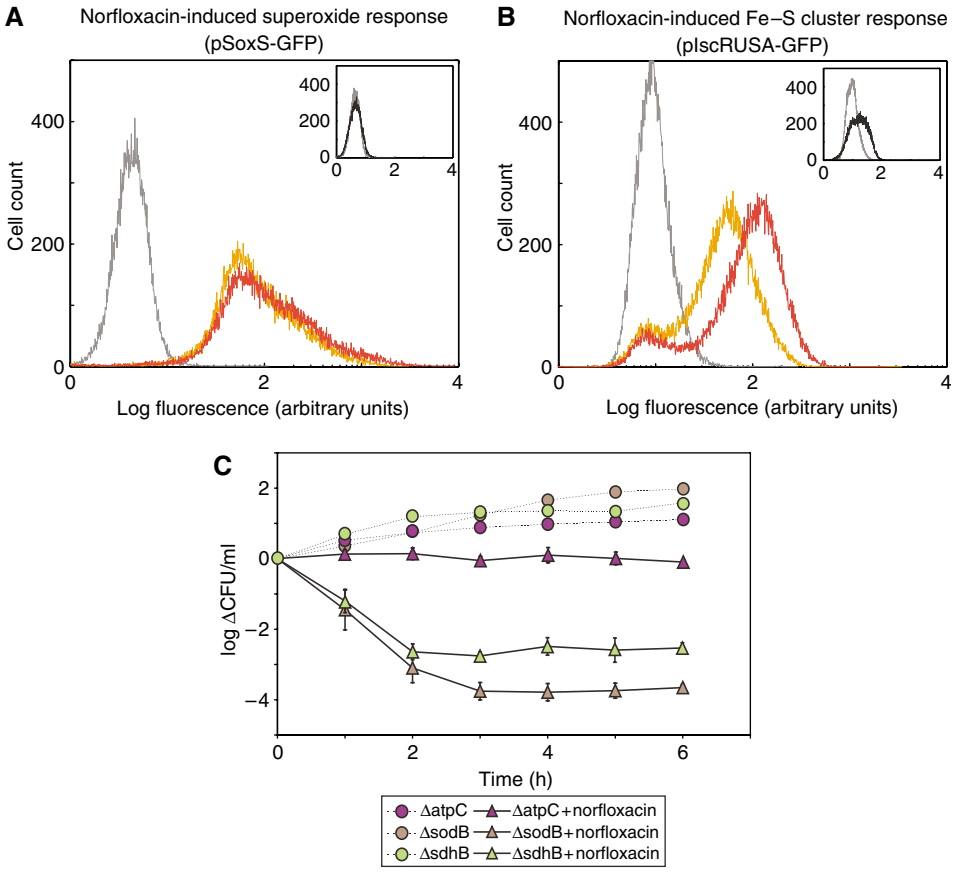

Figure 6 Gyrase inhibition induces the superoxide response and upregulation of iron–sulfur cluster assembly. (**A**) Induction of the superoxide response following gyrase inhibition. To confirm that the superoxide response was activated upon inhibition of gyrase, we employed the native *soxS* promoter in a promoter-GFP reporter gene construct, pSoxS-GFP; transcription from the *soxS* promoter is activated upon superoxide-based oxidation to the iron–sulfur cluster of the SoxR transcription factor. (**B**) Upregulation of Fe–S cluster assembly-related gene expression following gyrase inhibition. To determine whether expression of the Isc family of Fe–S cluster synthesis was increased upon inhibition of gyrase, we employed the native *iscRUSA* promoter in a promoter-GFP reporter gene construct, pIscRUSA-GFP; the *iscRUSA* promoter is autoregulated by IscR and is activated, for example, when Fe–S clusters are oxidized. Measurements of both constructs were taken, at single-cell resolution, using a flow cytometer. Representative fluorescence population distributions of norfloxacin-treated wild-type cultures before (time zero, gray) and after (3 h (orange) and 6 h (red)) gyrase inhibition are shown. The respective insets show representative control fluorescence measurements of uninhibited wild-type cultures at time zero (gray) and 6 h (black). (**C**) Log change in colony forming units per ml (CFU/ml) of BW25113 *E. coli* single-gene deletion strains. Growth curves for untreated deletion strains are shown for comparison purposes and are representative of growth in the absence of norfloxacin treatment. Survival data for treated samples are represented as mean ± s.d. Survival of Δ*atpC* (untreated, purple circles, dotted line; norfloxacin-treated, purple triangles, solid line), Δ*sdhB* (untreated, light green circles, dotted line; norfloxacin-treated, light green triangles, solid line) and Δ*sodB* cultures (untreated, brown circles, dotted line; norfloxacin treated, brown triangles, solid line) are shown.

E. coli encode distinct, yet compensatory, superoxide decomposition systems, and in addition to SodA, possess the Fur-regulated iron-superoxide dismutase, SodB (Fridovich, 1997; Dubrac and Touati, 2002). As SodB has been shown to be more proficient at protecting cytoplasmic Fe–S-containing proteins in *E. coli* (Hopkin *et al*, 1992), we next examined the effect of gyrase inhibition on a *sodB* deletion strain. Whereas Δ*sodB* and wild-type cells treated with norfloxacin showed similar growth behavior between the 0 and 2 h time points, Δ*sodB* cells exhibited sharply decreased survival over the final 4 h of the experiment, approaching our limit of detection (Figure 6C). The delay in the phenotypic response to norfloxacin treatment in this strain suggests that the generation of superoxide and superoxide-mediated oxidative damage does not occur immediately following gyrase inhibition. Rather, these data imply that oxidative damage is a secondary, yet quite deadly, effect of gyrase poisoning.

Previous work has established a link between DNA damage, SOS repair activity and bursting of ATP (Barbe *et al*, 1983; Dahan-Grobgeld *et al*, 1998). Given the connection between the respiratory electron-transport chain activity and superoxide generation (Imlay and Fridovich, 1991; Messner and Imlay, 2002), we hypothesized that a plausible biochemical explanation for superoxide formation and Fe–S oxidation after gyrase inhibitor-induced DNA damage was the increased production of ATP. To address this, we first measured cellular ATP levels in wild-type cells following gyrase poisoning by norfloxacin. Using a luciferase-based assay, we determined that at 1 h norfloxacin treatment induced a greater than 10^2-fold change in moles of ATP/cell when compared with untreated cells; this difference increased with the duration of the experiment (Supplementary Figure 9).

To further explore our hypothesis, we next studied the effect of disabling ATP synthase assembly, and thus genetic-level

Published online: March 13, 2007

uncoupling of oxidative phosphorylation, on gyrase inhibitor-mediated cell death. We challenged the majority of ATP synthase component genes with norfloxacin and observed increased survival (2-log increase in CFU/ml) in each case (Supplementary Figure 7). The most striking phenotypic change following norfloxacin application was exhibited by Δ*atpC* cultures, where we observed complete reversal of bactericidal activity. In this strain we observed a 3-log increase in survival relative to norfloxacin-treated wild-type cells (Figure 6C). These results clearly demonstrate that efficient norfloxacin-based killing is directly dependent on ATP, supporting published *in vitro* and *in vivo* findings (Kampranis and Maxwell, 1998; Li and Liu, 1998).

Lastly, we examined whether disabling the activity of TCA cycle component succinate dehydrogenase, also an aerobic respiratory electron-transport chain constituent, would affect cell survival following gyrase inhibition. The conversion of succinate to fumarate, catalyzed by succinate dehydrogenase, involves three Fe–S clusters (SdhB subunit) and has been shown to result in the generation of superoxide (Messner and Imlay, 2002); accordingly, we chose to study the effect of norfloxacin on the growth of Δ*sdhB* cells in order to reduce both the level of endogenous Fe–S cluster-bearing proteins and the production of superoxide. Compared with wild-type cells, norfloxacin treatment of Δ*sdhB* cells led to a 1-log increase in survival at 1 h and a more modest 0.5-log increase at 6 h. We suspect that this effect may be increased by knockout of additional Fe–S cluster-containing proteins and requires further investigation.

Together, these data suggest that gyrase inhibition promotes endogenous environmental changes that support the generation of superoxide radicals. Moreover, our findings help to provide an explanation for why the loss of superoxide dismutase activity (specifically that of SodB) enhances the killing effect of the gyrase poison, norfloxacin.

Hydroxyl radical production in Δ*atpC*, Δ*iscS* and Δ*sodB* cells

To validate the results of our genetic screening, we performed hydroxyl radical measurements, again using the reporter dye HPF, in the Δ*atpC,* Δ*iscS* and Δ*sodB* knockout strains. The largest detectable increase in hydroxyl radical-mediated fluorescence was observed following norfloxacin treatment of Δ*sodB* cells (Figure 7), consistent with the significantly increased cell death we saw following norfloxacin treatment (Figure 6B). In contrast, gyrase-inhibited Δ*iscS* cultures exhibited a reduced level of hydroxyl radicals compared with wild-type cultures (Figure 7). This was also consistent with our Δ*iscS* growth data (Figure 5A) and supports the notion that inefficient repair of Fe–S clusters will decrease the available ferrous iron by limiting redox cycling.

As anticipated, we were unable to detect a hydroxyl radical-mediated fluorescence shift in Δ*atpC* cultures treated with norfloxacin (Figure 7). This result, which is also consistent with phenotypic data (Figure 6C), strongly suggests a connection between gyrase inhibition, oxidative phosphorylation-driven superoxide production and hydroxyl radical production.

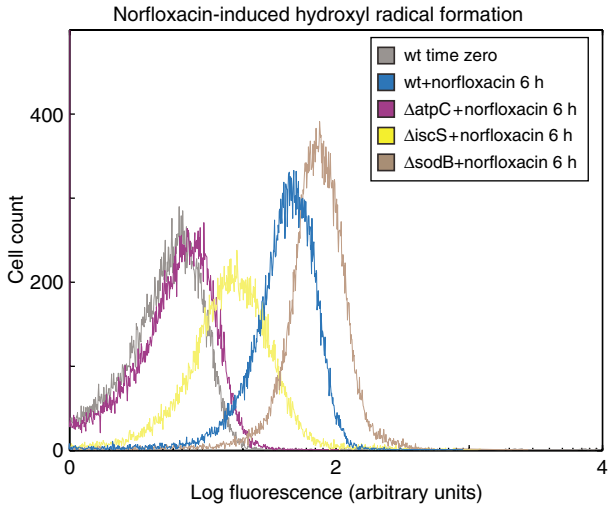

Figure 7 Generation of hydroxyl radicals in Δ*atpC*, Δ*iscS* and Δ*sodB* cells upon gyrase inhibition. Formation of oxidatively damaging hydroxyl radicals was measured using the highly specific fluorescent dye, HPF. Shown are representative flow cytometer-measured fluorescence population distributions of Δ*atpC* (purple), Δ*iscS* (yellow) and Δ*sodB* (brown) cultures taken 6 h after treatment with norfloxacin. For comparison, fluorescence measurements of wild-type cells before (time zero, gray) and after (6 h (blue)) gyrase inhibition are also shown.

Discussion

Gyrase inhibitors are known to induce cell death by stimulating DNA damage formation, impeding lesion repair and blocking replication processes (Drlica and Zhao, 1997; Couturier *et al*, 1998). In this study, we sought to identify additional mechanisms that directly or indirectly contribute to gyrase inhibitor-mediated cell killing. Here, we show that oxidative damage by superoxide and hydroxyl radicals contributes to bacterial cell death following gyrase poisoning. Superoxide, generated as a by-product of aerobic metabolism (Imlay and Fridovich, 1991), will attack proteins containing Fe–S clusters and oxidatively destabilize the cluster, often triggering the release of ferrous (II) iron (Keyer and Imlay, 1996). Based on our phenotypic and microarray analyses, we propose that repetitious Fe–S cluster oxidation and repair arises as a deadly and necessary adjunct that potentiates the killing ability of gyrase inhibitors. This cycling should serve to maintain a large pool of ferrous iron, which readily participates as a substrate in the Fenton reaction to produce hydroxyl radicals. Our results demonstrate that highly deleterious hydroxyl radicals, are in fact, generated through the Fenton reaction, upon gyrase poisoning. Based on our findings, we have constructed a model for a complementary bacterial cell death pathway (Figure 8), stimulated by gyrase inhibition, which involves ROS formation and a breakdown in iron regulatory dynamics.

In this work, we employed biochemical pathway and transcription factor regulatory classifications to identify functional modules within the transcriptional response in *E. coli* to gyrase poisoning and double-stranded DNA break formation.

Published online: March 13, 2007

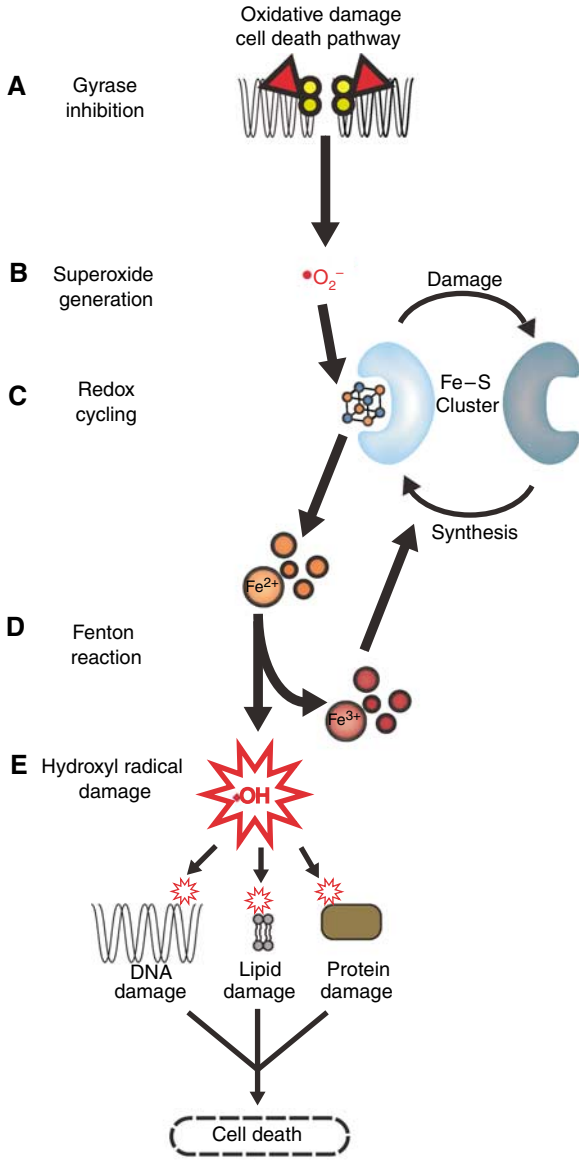

Figure 8 Oxidative damage cell death pathway model. A model for iron misregulation and reactive oxygen species generation following gyrase inhibition and DNA damage formation. (**A**) Gyrase inhibitors (red triangles), such as norfloxacin and CcdB, target DNA-bound gyrase (yellow circles). The resultant complex induces double-stranded breakage and loss of chromosomal supercoiling by preventing strand rejoining by the gyrase enzyme. (**B**) Gyrase poisoning promotes the generation of superoxide ($\bullet O_2^-$), which (**C**) oxidatively attacks iron–sulfur clusters (three-dimensional cube depicts [4Fe–4S] cluster; iron and sulfur are shown as orange and blue circles, respectively); sustained superoxide attack of iron–sulfur-containing proteins (light blue) leads to functional inactivation (dark blue), destabilization and iron leaching. (**D**) Repetitious oxidation and repair of clusters, or redox cycling, promotes iron misregulation and may serve to generate a cytoplasmic pool of 'free' ferrous (Fe^{2+}) iron. (**E**) Ferrous iron, via the Fenton reaction, rapidly catalyzes the formation of deleterious hydroxyl radicals ($\bullet$OH), which readily damage DNA, lipids and proteins; the Fenton reaction can thus take place at destabilized iron–sulfur clusters or where 'free' ferrous iron has accumulated. We propose that reactive oxygen species are generated via an oxygen-dependent death pathway that amplifies the primary effect of gyrase inhibition and contributes to cell death following gyrase poisoning.

This analysis revealed, as expected, that DNA lesion remediation and repair systems constitute a significant proportion of the quickest and highest responding gene set (Figure 2). Our microarray analysis also revealed enrichment for genes involved in oxidative stress responses, including the *soxRS* operon and *sodA*. Previous work has shown that a loss of chromosomal supercoiling, which occurs when gyrase is inhibited, results in the upregulation of oxidative phosphorylation and ATP bursting (Dahan-Grobgeld *et al*, 1998); we validate this finding in our present study, showing that gyrase poisoning rapidly results in a large increase in cellular ATP levels. The consequence of heightened ATP synthase and respiratory chain activity in an oxygen-rich environment is the expedited generation of the ROS, superoxide (Imlay, 2003). Here, we have shown that oxidative phosphorylation contributes to gyrase inhibitor-induced cell death, and that superoxide formation indeed occurs when gyrase is poisoned. With regard to oxidative phosphorylation, we found that blockage of succinate dehydrogenase activity led to a modest increase in cell viability whereas genetic-level uncoupling of ATP synthase activity resulted in a striking reduction of cell death following treatment with norfloxacin (Figure 6C). By employing a promoter-reporter gene fusion construct designed to respond to superoxide-related oxidation of SoxR, we were able to monitor the induction of the superoxide stress regulon as a function of gyrase inhibition (Figure 6A). Together, these findings suggest that our proposed oxidative damage cell death pathway (Figure 8) may exist as a maladaptive response to gyrase inhibitor-induced DNA damage in oxygen-rich environments.

Surprisingly, our systems biology analysis of the microarray data revealed that each component of the Fe–S cluster repair operon, *iscRUSA*, was significantly upregulated, and that the transcriptional regulator of this operon, IscR, was statistically enriched. This finding implied that prolonged exposure of Fe–S clusters to superoxide was occurring, as the Isc family of proteins has been shown to be critical to the repair of heavily oxidized Fe–S clusters (Djaman *et al*, 2004). This result also suggested that redox cycling, where heavily oxidized clusters are replaced with newly synthesized clusters, was occurring and would thus provide intracellularly abundant superoxide with a steady supply of new substrates. In light of our Δ*fur* and Δ*iscS* results, however, it is necessary to amend our initial hypothesis. It has previously been shown that deletion of the master iron regulator, Fur, results in increased levels of intracellular iron, a function of increased iron procurement system expression (Touati *et al*, 1995). Interestingly, it has also been shown that Fe–S cluster formation is related to Fur and that the overall number of Fe–S clusters is decreased in a Δ*fur* background (McHugh *et al*, 2003), similar to the effect on Fe–S cluster number in a Δ*iscS* background (Schwartz *et al*, 2000). Thus, our findings that cellular survival was increased following gyrase poisoning in Δ*fur* and Δ*iscS* cells imply that cell killing by gyrase inhibitors is intimately related to the number of intracellular Fe–S clusters and not just their status.

These results raise the question—whether the observed generation of hydroxyl radicals is related to repetitious breakdown and repair of damaged Fe–S clusters (and thus an increased endogenous level of unbound ferrous iron) or is it possible that hydroxyl radical production is actually taking

Published online: March 13, 2007

place at the exposed active sites of oxidatively-sensitive dehydratases (thus involving intact, yet perhaps unstable, 4Fe–4S clusters). The latter scenario has previously been proposed by Flint *et al* (1993), and it helps to explain the resistance to gyrase inhibition observed in Δ*fur*, and much more strikingly, in Δ*iscS* cells. This hypothesis would also help to explain why ectopic overexpression of Fur in the Δ*fur* background reverts norfloxacin-induced cell death to wild-type levels (Supplementary Figure 4). Moreover, this latter scenario would be still consistent with our iron chelator result, in which *o*-phenanthroline prevents hydroxyl radical formation by sequestering any Fenton-reactive exposed iron in dehydratase Fe–S clusters.

It is quite likely that these events would induce global iron misregulation and a disruption in iron metabolism. Indeed, our engineered iron regulatory reporter gene construct revealed that a breakdown in iron regulatory dynamics occurs when gyrase is inhibited (Figures 5B). Specifically, increased Fur-related GFP expression implies less Fur–Fe(II) complexes; however, this does not necessarily signify low internal concentrations of Fe(II) and may reflect an internal perception that increased uptake is necessary, or simply a sign that internal iron is 'stuck' in a redox cycle of Fe–S cluster oxidation and repair and cannot be recognized and/or bound by Fur. It is plausible then that the misregulation of Fur-controlled iron uptake, utilization and maintenance genes may serve to amplify the oxidative potential by sustaining a pool of Fenton-ready 'free iron'.

As noted above, our proposed oxidative damage cell death pathway (Figure 8) appears to be a maladaptive response by aerobically growing *E. coli* to DNA gyrase inhibition and DNA damage formation by both a synthetic antibiotic and an endogenous toxin. The biochemical reliance of bacteria on Fe–S catalysis, evolutionarily related to the oxygen-free and iron- and sulfur-rich environment that existed billions of years ago (Johnson *et al*, 2005; Imlay, 2006), has predisposed these organisms to oxidative damage. This 'backdoor' appears to be exploited by gyrase-inhibiting bactericidal agents in exacting cell death, which may explain the dependence of quinolone antibiotics (i.e. ofloxacin and ciprofloxacin; Morrissey and Smith, 1994) on oxygen and aerobic growth for bactericidal activity. Our findings may contribute to the development of novel antibacterial therapies (Walsh, 2003; McAdams *et al*, 2004) that exhibit more efficient bactericidal activity.

It is interesting to note that the *isc* operon, which we implicate in gyrase inhibitor-mediated iron misregulation and redox cycling, is highly conserved in eukaryotes and is involved in mitochondrial Fe–S cluster assembly (Muhlenhoff and Lill, 2000; Johnson *et al*, 2005). Moreover, the production of ROS as a kill signal has parallels in apoptosis, and the relationship between ROS, specifically hydroxyl radicals, and mitochondrial breakdown is well established (Zamzami *et al*, 1995; Jacobson, 1996; Green and Reed, 1998; Madeo *et al*, 1999; Simon *et al*, 2000; Brookes *et al*, 2004). Given these connections, it is thus tempting to consider that the maladaptive response to gyrase poisoning by norfloxacin and CcdB we observe in *E. coli* may have evolved into targeted and efficient killing programs in higher order organisms, including DNA damage-induced apoptosis in eukaryotes.

Materials and methods

Plasmid construction, cell strains and reagents

Basic molecular biology techniques were implemented as previously described (Sambrook and Russell, 2001). All plasmids were constructed using restriction endonucleases and T4 DNA ligase from New England Biolabs. For cloning purposes, we transformed plasmids into the *E. coli* strain XL-10 (Stratagene; Tet^r Δ(mcrA)183, Δ(mcrCB-hsdSMR-mrr)173, endA1, supE44, thi-1, recA1, gyrA96, relA1, lac Hte (F proAB lacIq ZDM15 Tn10 (Tet^r) Amy Cam^r) using standard heat-shock protocols (Sambrook and Russell, 2001). All cells were grown in selective medium: Luria–Bertani (LB) media (Fisher) supplemented with 30 μg/ml of kanamycin (Fisher). Plasmid isolation was performed using the QIAprep Spin Miniprep kits (Qiagen). Subcloning was confirmed by restriction analysis. Plasmid modifications were verified by sequencing using the PE Biosystem ABI Prism 377 sequencer.

Our riboregulated CcdB expression plasmid was built according to our published design (Isaacs *et al*, 2004). The *ccdB* gene was amplified by PCR from F plasmid-containing XL-10 cells using the PTC-200 PCR machine (Bio-Rad) with the Expand Long Template PCR System (Roche). Oligonucleotide primers were purchased from Integrated DNA Technologies.

Transcription of *cis*-repressed *ccdB* mRNA was controlled using the $P_{LlacO-1}$ promoter (Lutz and Bujard, 1997), a modified version of the native bacteriophage λ P_L promoter containing two LacI operator sites; transcription was thus induced by addition of IPTG (Fisher). The P_{BAD} promoter regulates the production of the *trans*-activating RNA necessary for CcdB toxin translation; CcdB translation was induced by the addition of arabinose. This system is described in detail in Supplementary information.

Our DNA damage and iron regulation sensors were based on the design of the $P_{LlacO-1}$ promoter (Lutz and Bujard, 1997), a synthetic variant of the native bacteriophage λ P_L promoter. In this design, LacI operator sites were inserted near both the −10 and −35 sequences required for RNA polymerase binding, such that LacI binding would sterically inhibit transcription. In our study, PCR was used to build each novel promoter, which employed LexA and Fur operator sites to regulate expression, respectively, of the green fluorescent protein gene, *gfpmut3b* (Cormack *et al*, 1996).

To construct our superoxide response sensor, we PCR-amplified the native *soxS* promoter from XL-10 cells and cloned it upstream of the *gfpmut3b* gene. To construct our Fe–S cluster response (IscR) sensor, we PCR-amplified the native *iscRUSA* promoter from XL-10 cells and cloned it upstream of the *gfpmut3b* gene.

Growth analysis

In our initial experiments, we compared the growth of untreated, norfloxacin-treated (250 ng/ml), CcdB− (uninduced cultures containing the *ccdB* riboregulator) and CcdB+ (induced cultures containing the *ccdB* riboregulator) wild-type BW25113 ($lacI^q$ $rrnB_{T14}$ $\Delta lacZ_{WJ16}$ *hsdR514* $\Delta araBAD_{AH33}$ $\Delta rhaBAD_{LD78}$) cultures. In our specific single-gene knockout experiments, we studied the growth of deletion strains contained in a BW25113 deletion library (Baba *et al*, 2006).

For all experiments, cells were grown overnight, then diluted 1:1000 in 50 ml LB (+30 μg/ml kanamycin for CcdB-expressing cells) for collection of OD_{600} and CFU/ml samples. For those experiments performed in the presence of iron chelator, growth media were supplemented with 100 μM *o*-phenanthroline (Sigma). CcdB+ cultures were induced by the addition of 1 mM IPTG and 0.25% arabinose when they reached an OD_{600} of 0.3–0.4. Measurements of OD_{600} were taken using a SPECTRAFluor Plus (Tecan). For CFU/ml measurements, 100 μl of culture was collected, washed twice with filtered 1 × PBS, pH 7.2 (Fisher) and then serially diluted in 1 × PBS. A 10 μl portion of each dilution was plated onto individual wells of a 24-well plate, with each well containing 1 ml of LB agar (Fisher) (+30 μg/ml kanamycin for CcdB-expressing cells), and the plate was incubated overnight at 37°C. Only dilutions that yielded between 20 and 100 colonies were counted and CFU/ml values were calculated using the formula ((# of colonies)(dilution factor))/0.01 ml.

Promoter-reporter gene construct experiments using flow cytometry

To monitor the occurrence of DNA damage, oxidative damage to Fe–S clusters and changes in iron regulation, we employed engineered sensors that respond to these biochemical events by activating expression of *gfpmut3b*. All data were collected using a Becton Dickinson FACSCalibur flow cytometer (Becton Dickinson) with a 488-nm argon laser and a 515–545 nm emission filter (FL1) at low flow rate. The following PMT voltage settings were used: E00 (FSC), 300 (SSC) and 700 (FL1). Calibrite Beads (Becton Dickinson) were used for instrument calibration.

Flow data were converted to ASCII format using MFI (E Martz, University of Massachusetts, Amherst) and processed with MATLAB (MathWorks) to construct figures. At least 50 000 cells were collected for each sample.

In all experiments, cells were grown overnight and then diluted 1:1000 in 50 ml LB supplemented with 100 μg/ml ampicillin (Fisher) (+30 μg/ml kanamycin for CcdB-expressing cells). CcdB expression was induced by addition of 1 mM IPTG and 0.25% arabinose at an OD_{600} of 0.3–0.4; 250 ng/ml norfloxacin was added to drug-treated cultures at an OD_{600} of 0.3–0.4. For those experiments performed in the presence of iron chelator, growth media were supplemented with 100 μM *o*-phenanthroline (Sigma). For those experiments performed in the presence of paraquat, growth media were supplemented with 10 μM paraquat (Acros Organics). Samples were taken immediately before induction (time zero), then every hour for 6 h. At each time point, approximately 10^6 cells were collected, washed once and resuspended in filtered 1 × PBS, pH 7.2 (Fisher) and measured on the flow cytometer.

Gene expression analysis

We compared the microarray-determined mRNA profiles of *E. coli* BW25113 cultures in response to CcdB and norfloxacin with those of untreated cultures. For all experiments, cells were grown overnight and then diluted 1:1000 in 50 ml LB (+30 μg/ml kanamycin for CcdB-expressing cells) for collection of total RNA. CcdB-expressing cultures were induced with 1 mM IPTG and 0.25% arabinose at an OD_{600} of 0.3–0.4; 250 ng/ml norfloxacin was added to norfloxacin-treated cultures at an OD_{600} of 0.3–0.4. Untreated cultures were grown in LB with no exogenous inducers or antibiotics added. Samples for microarray analysis were taken immediately before induction (time zero) and then at 30, 60 and 120 min post-induction.

Total RNA was obtained using the RNeasy Protect Bacteria Mini kit (Qiagen) according to the manufacturer's instructions. RNAprotect (Qiagen) was added to culture samples, which were then pelleted by centrifugation at 3000 *g* for 15 min and stored overnight at −80°C. Total RNA was then extracted using the RNeasy kit and samples were DNase-treated using DNA-*free* (Ambion). Sample concentration was estimated using the ND-1000 spectrophotometer (NanoDrop).

cDNA was prepared from 10 μg total RNA by random primed reverse transcription using SuperScript II (Invitrogen). The RNA was digested by adding 1 M NaOH and then incubating at 65°C for 30 min. The mixture was neutralized by the addition of 1 M HCl. The cDNA was purified using a QIAquick PCR purification column (Qiagen) following the manufacturer's protocol. The cDNA was fragmented to a size range of 50–200 bases with DNase I (0.6 U/μg cDNA) at 37°C for 10 min, followed by inactivation of the enzyme at 98°C for 10 min. Subsequently, the fragmented cDNA was biotin labeled using an Enzo BioArray Terminal Labeling kit with Biotin-ddUTP (Enzo Scientific). Fragmented, biotinylated cDNA was hybridized to Affymetrix *E. coli* Antisense Genome arrays for 16 h at 45°C and 60 r.p.m.

Following hybridization, arrays were washed and stained according to the standard Antibody Amplification for ProkaryoticTargets protocol (Affymetrix). This consisted of a wash with non-stringent buffer, followed by a wash with stringent buffer, a stain with strepavidin, a wash with non-stringent buffer, a stain with biotinylated anti-strepavidin antibody, a stain with strepavidin–phycoerythrin and a final wash with non-stringent buffer. The stained GeneChip arrays were scanned at 532 nm using an Affymetrix GeneChip Scanner 3000. The scanned images were scaled and quantified using GCOS v1.2 software.

The resulting *.CEL files were combined with *.CEL files from arrays that comprise the M3D compendium (T Gardner, Boston University, http://m3d.bu.edu) and RMA-normalized (Irizarry *et al*, 2003) for a total of 505 RMA-normalized *E. coli* expression arrays. Subsequently, we subtracted the mean normalized expression for each gene from its respective normalized expression for each individual experiment and then divided it by the respective standard deviation of each gene across all experiments. This converts the expression values for all genes across all experiments into estimated *z*-scores based on the observed expression distribution for each gene across all experiments in the M3D compendium.

To determine statistically significant changes in gene expression owing to norfloxacin treatment or CcdB expression, we subtracted the expression *z*-score of each gene in our uninduced control data set from the corresponding *z*-score in our perturbed (norfloxacin-treated or CcdB-expressing) sample data set. This was carried out for each experimental time point (0, 30, 60, 120 and 180 min), for example, the *z*-score of *recA* expression from our uninduced sample at 30 min was subtracted from the *recA z*-score from our norfloxacin-treated sample at 30 min. This allowed us to determine the difference in expression between an uninduced control set and a gyrase inhibitor-treated data set in terms of units of standard deviation, a robust metric. A gene was considered to have significantly changed expression when its *z*-score difference was greater than two units of standard deviation, with the sign determining overexpression and underexpression. Finally, as a separate analysis of differential gene expression, and to reduce the dimensionality of these data, we conflated the difference of *z*-scores across all time points (a weighted *Z*-test, essentially combining values from multiple tests of the same hypothesis) by utilizing the formula, $Z_{average}$=sum_t (Z_t)/sqrt(t) (Whitlock, 2005).

Following the identification of significantly changed genes at each time point, we performed functional enrichment using GO classification terms (Ashburner *et al*, 2000; Camon *et al*, 2004) and the GO::TermFinder program (Boyle *et al*, 2004). In doing this, we were able to group genes by GO annotated pathways and determine statistical significance. We next utilized the transcription factor regulatory information contained in RegulonDB (version 4) (Salgado *et al*, 2006) together with a transcriptional regulatory map assembled by the program, CLR (Faith *et al*, 2007). Using both sets of information, we were able to categorize significantly changed genes into functional units to monitor coordinated responses.

Hydroxyl radical measurements

To detect hydroxyl radical formation following norfloxacin treatment or CcdB expression, we used the fluorescent reporter dye, 3′-(*p*-hydroxyphenyl) fluorescein (HPF; Invitrogen), which is oxidized by hydroxyl radicals with high specificity. All data were collected using the Becton Dickinson FACSCalibur flow cytometer described above (Becton Dickinson). The following PMT voltage settings were used: E00 (FSC), 300 (SSC) and 825 (FL1). Calibrite Beads (Becton Dickinson) were used for instrument calibration. Flow data were collected, converted and analyzed as above.

In all experiments, cells were grown overnight, then diluted 1:1000 in 50 ml LB (+30 μg/ml kanamycin for CcdB-expressing cells) and supplemented with 5 μM HPF. For those experiments involving iron chelator, growth media were supplemented with 100 μM *o*-phenanthroline. CcdB expression was induced by the addition of 1 mM IPTG and 0.25% arabinose at an OD_{600} of 0.3–0.4; 250 ng/ml norfloxacin was added to drug-treated cultures at an OD_{600} of 0.3–0.4. Samples were collected and prepared for flow cytometry as above.

ATP measurements

To monitor the increase in ATP formation following gyrase inhibition, we used the BacTiter-Glo Microbial Cell Viability Assay (Promega), a firefly luciferase bioluminescence-based assay, according to the manufacturer's instructions. Luminescence measurements were taken using a SPECTRAFluor Plus (Tecan). ATP disodium salt (MP

Biomedicals) was used as a control to generate a standard curve, according to the manufacturer's instructions.

In all experiments, cells were grown overnight and then diluted 1:1000 in 50 ml LB (+30 μg/ml kanamycin for CcdB-expressing cells). CcdB expression was induced by the addition of 1 mM IPTG and 0.25% arabinose at an OD_{600} of 0.3–0.4; 250 ng/ml norfloxacin was added to drug-treated cultures at an OD_{600} of 0.3–0.4. At each time point, 100 μl of each culture was taken and incubated with 100 μl BacTiter-Glo reagent for 10 min, at 25°C, with shaking; samples were also taken simultaneously for CFU/ml measurements. ATP values (in moles) were calculated based on the standard curve, and moles ATP per cell values were calculated by dividing moles ATP to CFU/ml measurements.

Supplementary information

Supplementary information is available at the *Molecular Systems Biology* website (www.nature.com/msb).

Acknowledgements

This work was supported by the National Science Foundation and the United States Department of Energy. We are grateful to Marc Lenburg and Norman Gerry for performing microarray experiments, and to Hirotada Mori and colleagues for their donation of the BW25113 *E. coli* knockout library. We thank Iris Keren, Guillaume Cottarel, Jamey Wierzbowski and Philina Lee for critical review of the manuscript. We also thank the anonymous reviewers of this work for their important advice and suggestions.

References

Andrews SC, Robinson AK, Rodriguez-Quinones F (2003) Bacterial iron homeostasis. *FEMS Microbiol Rev* **27:** 215–237

Aruoma OI, Halliwell B, Dizdaroglu M (1989) Iron ion-dependent modification of bases in DNA by the superoxide radical-generating system hypoxanthine/xanthine oxidase. *J Biol Chem* **264:** 13024–13028

Asad NR, Leitao AC (1991) Effects of metal ion chelators on DNA strand breaks and inactivation produced by hydrogen peroxide in *Escherichia coli*: detection of iron-independent lesions. *J Bacteriol* **173:** 2562–2568

Ashburner M, Ball CA, Blake JA, Botstein D, Butler H, Cherry JM, Davis AP, Dolinski K, Dwight SS, Eppig JT, Harris MA, Hill DP, Issel-Tarver L, Kasarskis A, Lewis S, Matese JC, Richardson JE, Ringwald M, Rubin GM, Sherlock G (2000) Gene ontology: tool for the unification of biology. The Gene Ontology Consortium. *Nat Genet* **25:** 25–29

Baba T, Ara T, Hasegawa M, Takai Y, Okumura Y, Baba M, Datsenko KA, Tomita M, Wanner BL, Mori H (2006) Construction of *Escherichia coli* K-12 in-frame, single-gene knockout mutants: the Keio collection. *Mol Syst Biol* **2**:2006.0008

Balasubramanian B, Pogozelski WK, Tullius TD (1998) DNA strand breaking by the hydroxyl radical is governed by the accessible surface areas of the hydrogen atoms of the DNA backbone. *Proc Natl Acad Sci USA* **95:** 9738–9743

Barbe J, Villaverde A, Guerrero R (1983) Evolution of cellular ATP concentration after UV-mediated induction of SOS system in *Escherichia coli*. *Biochem Biophys Res Commun* **117:** 556–561

Bernard P, Couturier M (1992) Cell killing by the F plasmid CcdB protein involves poisoning of DNA-topoisomerase II complexes. *J Mol Biol* **226:** 735–745

Bernard P, Kezdy KE, Van Melderen L, Steyaert J, Wyns L, Pato ML, Higgins PN, Couturier M (1993) The F plasmid CcdB protein induces efficient ATP-dependent DNA cleavage by gyrase. *J Mol Biol* **234:** 534–541

Boyle EI, Weng S, Gollub J, Jin H, Botstein D, Cherry JM, Sherlock G (2004) GO::TermFinder—open source software for accessing Gene Ontology information and finding significantly enriched Gene Ontology terms associated with a list of genes. *Bioinformatics* **20:** 3710–3715

Brookes PS, Yoon Y, Robotham JL, Anders MW, Sheu SS (2004) Calcium, ATP, and ROS: a mitochondrial love–hate triangle. *Am J Physiol Cell Physiol* **287:** C817–833

Camon E, Magrane M, Barrell D, Lee V, Dimmer E, Maslen J, Binns D, Harte N, Lopez R, Apweiler R (2004) The Gene Ontology Annotation (GOA) Database: sharing knowledge in Uniprot with Gene Ontology. *Nucleic Acids Res* **32:** D262–266

Champoux JJ (2001) DNA topoisomerases: structure, function, and mechanism. *Annu Rev Biochem* **70:** 369–413

Chen CR, Malik M, Snyder M, Drlica K (1996) DNA gyrase and topoisomerase IV on the bacterial chromosome: quinolone-induced DNA cleavage. *J Mol Biol* **258:** 627–637

Clarke TE, Tari LW, Vogel HJ (2001) Structural biology of bacterial iron uptake systems. *Curr Top Med Chem* **1:** 7–30

Cormack BP, Valdivia RC, Falkow S (1996) FACS-optimized mutants of the green fluorescent protein (GFP). *Gene* **173:** 33–38

Courcelle J, Hanawalt PC (2003) RecA-dependent recovery of arrested DNA replication forks. *Annu Rev Genet* **37:** 611–646

Couturier M, Bahassi el M, Van Melderen L (1998) Bacterial death by DNA gyrase poisoning. *Trends Microbiol* **6:** 269–275

Cox MM, Goodman MF, Kreuzer KN, Sherratt DJ, Sandler SJ, Marians KJ (2000) The importance of repairing stalled replication forks. *Nature* **404:** 37–41

Cozzarelli NR (1980) DNA gyrase and the supercoiling of DNA. *Science* **207:** 953–960

Critchlow SE, O'Dea MH, Howells AJ, Couturier M, Gellert M, Maxwell A (1997) The interaction of the F plasmid killer protein, CcdB, with DNA gyrase: induction of DNA cleavage and blocking of transcription. *J Mol Biol* **273:** 826–839

Dahan-Grobgeld E, Livneh Z, Maretzek AF, Polak-Charcon S, Eichenbaum Z, Degani H (1998) Reversible induction of ATP synthesis by DNA damage and repair in *Escherichia coli*. *In vivo* NMR studies. *J Biol Chem* **273:** 30232–30238

de Mello Filho AC, Meneghini R (1985) Protection of mammalian cells by *o*-phenanthroline from lethal and DNA-damaging effects produced by active oxygen species. *Biochim Biophys Acta* **847:** 82–89

Djaman O, Outten FW, Imlay JA (2004) Repair of oxidized iron–sulfur clusters in *Escherichia coli*. *J Biol Chem* **279:** 44590–44599

Drlica K, Zhao X (1997) DNA gyrase, topoisomerase IV, and the 4-quinolones. *Microbiol Mol Biol Rev* **61:** 377–392

Dubrac S, Touati D (2002) Fur-mediated transcriptional and post-transcriptional regulation of FeSOD expression in *Escherichia coli*. *Microbiology* **148:** 147–156

Elledge SJ, Walker GC (1983) Proteins required for ultraviolet light and chemical mutagenesis. Identification of the products of the umuC locus of *Escherichia coli*. *J Mol Biol* **164:** 175–192

Escolar L, Perez-Martin J, de Lorenzo V (1999) Opening the iron box: transcriptional metalloregulation by the Fur protein. *J Bacteriol* **181:** 6223–6229

Faith JJ, Hayete B, Thaden JT, Mogno I, Wierzbowski J, Cottarel G, Kasif S, Collins JJ, Gardner TS (2007) Large-scale mapping and validation of *Escherichia coli* transcriptional regulation from a compendium of expression profiles. *PLoS Biol* **5:** e8

Farr SB, Kogoma T (1991) Oxidative stress responses in *Escherichia coli* and *Salmonella typhimurium*. *Microbiol Rev* **55:** 561–585

Flint DH, Tuminello JF, Emptage MH (1993) The inactivation of Fe–S cluster containing hydro-lyases by superoxide. *J Biol Chem* **268:** 22369–22376

Fridovich I (1997) Superoxide anion radical (O_2^{-}.), superoxide dismutases, and related matters. *J Biol Chem* **272:** 18515–18517

Friedberg EC, Walker GC, Siede W, Wood RD, Schultz RA, Ellenberger T (2005) *DNA Repair and Mutagenesis*. Washington, DC: ASM Press

Gaudu P, Moon N, Weiss B (1997) Regulation of the soxRS oxidative stress regulon. Reversible oxidation of the Fe–S centers of SoxR *in vivo*. *J Biol Chem* **272:** 5082–5086

Gellert M (1981) DNA topoisomerases. *Annu Rev Biochem* **50:** 879–910

Gellert M, Mizuuchi K, O'Dea MH, Nash HA (1976) DNA gyrase: an enzyme that introduces superhelical turns into DNA. *Proc Natl Acad Sci USA* **73:** 3872–3876

Giel JL, Rodionov D, Liu M, Blattner FR, Kiley PJ (2006) IscR-dependent gene expression links iron–sulphur cluster assembly to the control of O_2-regulated genes in *Escherichia coli*. *Mol Microbiol* **60:** 1058–1075

Green DR, Reed JC (1998) Mitochondria and apoptosis. *Science* **281:** 1309–1312

Hanawalt PC (1966) The UV sensitivity of bacteria: its relation to the DNA replication cycle. *Photochem Photobiol* **5:** 1–12

Henle ES, Han Z, Tang N, Rai P, Luo Y, Linn S (1999) Sequence-specific DNA cleavage by Fe_2^+-mediated Fenton reactions has possible biological implications. *J Biol Chem* **274:** 962–971

Hidalgo E, Leautaud V, Demple B (1998) The redox-regulated SoxR protein acts from a single DNA site as a repressor and an allosteric activator. *EMBO J* **17:** 2629–2636

Hopkin KA, Papazian MA, Steinman HM (1992) Functional differences between manganese and iron superoxide dismutases in *Escherichia coli* K-12. *J Biol Chem* **267:** 24253–24258

Imlay JA (2003) Pathways of oxidative damage. *Annu Rev Microbiol* **57:** 395–418

Imlay JA (2006) Iron–sulphur clusters and the problem with oxygen. *Mol Microbiol* **59:** 1073–1082

Imlay JA, Fridovich I (1991) Superoxide production by respiring membranes of *Escherichia coli*. *Free Radic Res Commun* **12–13** (Part 1)**:** 59–66

Imlay JA, Linn S. (1988) DNA damage and oxygen radical toxicity. *Science* **240:** 1302–1309

Imlay JA, Chin SM, Linn S (1988) Toxic DNA damage by hydrogen peroxide through the Fenton reaction *in vivo* and *in vitro*. *Science* **240:** 640–642

Irizarry RA, Hobbs B, Collin F, Beazer-Barclay YD, Antonellis KJ, Scherf U, Speed TP (2003) Exploration, normalization, and summaries of high density oligonucleotide array probe level data. *Biostatistics* **4:** 249–264

Isaacs FJ, Dwyer DJ, Ding C, Pervouchine DD, Cantor CR, Collins JJ (2004) Engineered riboregulators enable post-transcriptional control of gene expression. *Nat Biotechnol* **22:** 841–847

Jacobson MD (1996) Reactive oxygen species and programmed cell death. *Trends Biochem Sci* **21:** 83–86

Jaffe A, Ogura T, Hiraga S (1985) Effects of the ccd function of the F plasmid on bacterial growth. *J Bacteriol* **163:** 841–849

Johnson DC, Dean DR, Smith AD, Johnson MK (2005) Structure, function, and formation of biological iron–sulfur clusters. *Annu Rev Biochem* **74:** 247–281

Kampranis SC, Maxwell A (1998) The DNA gyrase–quinolone complex. ATP hydrolysis and the mechanism of DNA cleavage. *J Biol Chem* **273:** 22615–22626

Kenyon CJ, Walker GC (1980) DNA-damaging agents stimulate gene expression at specific loci in *Escherichia coli*. *Proc Natl Acad Sci USA* **77:** 2819–2823

Keyer K, Imlay JA (1996) Superoxide accelerates DNA damage by elevating free-iron levels. *Proc Natl Acad Sci USA* **93:** 13635–13640

Kreuzer KN, Cozzarelli NR (1979) *Escherichia coli* mutants thermosensitive for deoxyribonucleic acid gyrase subunit A: effects on deoxyribonucleic acid replication, transcription, and bacteriophage growth. *J Bacteriol* **140:** 424–435

Li TK, Liu LF (1998) Modulation of gyrase-mediated DNA cleavage and cell killing by ATP. *Antimicrob Agents Chemother* **42:** 1022–1027

Liochev SI, Fridovich I (1999) Superoxide and iron: partners in crime. *IUBMB Life* **48:** 157–161

Liochev SL (1996) The role of iron–sulfur clusters in *in vivo* hydroxyl radical production. *Free Radic Res* **25:** 369–384

Little JW (1991) Mechanism of specific LexA cleavage: autodigestion and the role of RecA coprotease. *Biochimie* **73:** 411–421

Little JW, Mount DW (1982) The SOS regulatory system of *Escherichia coli*. *Cell* **29:** 11–22

Lutz R, Bujard H (1997) Independent and tight regulation of transcriptional units in *Escherichia coli* via the LacR/O, the TetR/O and AraC/I1-I2 regulatory elements. *Nucleic Acids Res* **25:** 1203–1210

Madeo F, Frohlich E, Ligr M, Grey M, Sigrist SJ, Wolf DH, Frohlich KU (1999) Oxygen stress: a regulator of apoptosis in yeast. *J Cell Biol* **145:** 757–767

Maki S, Takiguchi S, Miki T, Horiuchi T (1992) Modulation of DNA supercoiling activity of *Escherichia coli* DNA gyrase by F plasmid proteins. Antagonistic actions of LetA (CcdA) and LetD (CcdB) proteins. *J Biol Chem* **267:** 12244–12251

McAdams HH, Srinivasan B, Arkin AP (2004) The evolution of genetic regulatory systems in bacteria. *Nat Rev Genet* **5:** 169–178

McBride TJ, Preston BD, Loeb LA (1991) Mutagenic spectrum resulting from DNA damage by oxygen radicals. *Biochemistry* **30:** 207–213

McEntee K (1977) Protein X is the product of the recA gene of *Escherichia coli*. *Proc Natl Acad Sci USA* **74:** 5275–5279

McHugh JP, Rodriguez-Quinones F, Abdul-Tehrani H, Svistunenko DA, Poole RK, Cooper CE, Andrews SC (2003) Global iron-dependent gene regulation in *Escherichia coli*. A new mechanism for iron homeostasis. *J Biol Chem* **278:** 29478–29486

Messner KR, Imlay JA (2002) Mechanism of superoxide and hydrogen peroxide formation by fumarate reductase, succinate dehydrogenase, and aspartate oxidase. *J Biol Chem* **277:** 42563–42571

Miki T, Park JA, Nagao K, Murayama N, Horiuchi T (1992) Control of segregation of chromosomal DNA by sex factor F in *Escherichia coli*. Mutants of DNA gyrase subunit A suppress letD (ccdB) product growth inhibition. *J Mol Biol* **225:** 39–52

Mizuuchi K, O'Dea MH, Gellert M (1978) DNA gyrase: subunit structure and ATPase activity of the purified enzyme. *Proc Natl Acad Sci USA* **75:** 5960–5963

Morrissey I, Smith JT (1994) The importance of oxygen in the killing of bacteria by ofloxacin and ciprofloxacin. *Microbios* **79:** 43–53

Muhlenhoff U, Lill R (2000) Biogenesis of iron–sulfur proteins in eukaryotes: a novel task of mitochondria that is inherited from bacteria. *Biochim Biophys Acta* **1459:** 370–382

Norkin LC (1970) Marker-specific effects in genetic recombination. *J Mol Biol* **51:** 633–655

Nunoshiba T, Obata F, Boss AC, Oikawa S, Mori T, Kawanishi S, Yamamoto K (1999) Role of iron and superoxide for generation of hydroxyl radical, oxidative DNA lesions, and mutagenesis in *Escherichia coli*. *J Biol Chem* **274:** 34832–34837

Outten FW, Djaman O, Storz G (2004) A suf operon requirement for Fe–S cluster assembly during iron starvation in *Escherichia coli*. *Mol Microbiol* **52:** 861–872

Rai P, Cole TD, Wemmer DE, Linn S (2001) Localization of Fe(2 +) at an RTGR sequence within a DNA duplex explains preferential cleavage by Fe(2 +) and H_2O_2. *J Mol Biol* **312:** 1089–1101

Reece RJ, Maxwell A (1991) DNA gyrase: structure and function. *Crit Rev Biochem Mol Biol* **26:** 335–375

Salgado H, Gama-Castro S, Peralta-Gil M, Diaz-Peredo E, Sanchez-Solano F, Santos-Zavaleta A, Martinez-Flores I, Jimenez-Jacinto V, Bonavides-Martinez C, Segura-Salazar J, Martinez-Antonio A, Collado-Vides J (2006) RegulonDB (version 5.0): *Escherichia coli* K-12 transcriptional regulatory network, operon organization, and growth conditions. *Nucleic Acids Res* **34:** D394–D397

Sambrook J, Russell DW (2001) *Molecular Cloning: A Laboratory Manual*. Cold Spring Harbor, NY: Cold Spring Harbor Laboratory Press

Schleif R (1972) Fine-structure deletion map of the *Escherichia coli* L-arabinose operon. *Proc Natl Acad Sci USA* **69:** 3479–3484

Schwartz CJ, Djaman O, Imlay JA, Kiley PJ (2000) The cysteine desulfurase, IscS, has a major role in *in vivo* Fe–S cluster formation in *Escherichia coli*. *Proc Natl Acad Sci USA* **97:** 9009–9014

Published online: March 13, 2007

Schwartz CJ, Giel JL, Patschkowski T, Luther C, Ruzicka FJ, Beinert H, Kiley PJ (2001) IscR, an Fe–S cluster-containing transcription factor, represses expression of *Escherichia coli* genes encoding Fe–S cluster assembly proteins. *Proc Natl Acad Sci USA* **98:** 14895–14900

Setsukinai K, Urano Y, Kakinuma K, Majima HJ, Nagano T (2003) Development of novel fluorescence probes that can reliably detect reactive oxygen species and distinguish specific species. *J Biol Chem* **278:** 3170–3175

Simon HU, Haj-Yehia A, Levi-Schaffer F (2000) Role of reactive oxygen species (ROS) in apoptosis induction. *Apoptosis* **5:** 415–418

Sugino A, Higgins NP, Cozzarelli NR (1980) DNA gyrase subunit stoichiometry and the covalent attachment of subunit A to DNA during DNA cleavage. *Nucleic Acids Res* **8:** 3865–3874

Sutton MD, Walker GC (2001) Managing DNA polymerases: coordinating DNA replication, DNA repair, and DNA recombination. *Proc Natl Acad Sci USA* **98:** 8342–8349

Touati D (2000) Iron and oxidative stress in bacteria. *Arch Biochem Biophys* **373:** 1–6

Touati D, Jacques M, Tardat B, Bouchard L, Despied S (1995) Lethal oxidative damage and mutagenesis are generated by iron in delta fur mutants of *Escherichia coli*: protective role of superoxide dismutase. *J Bacteriol* **177:** 2305–2314

Walker GC (1984) Mutagenesis and inducible responses to deoxyribonucleic acid damage in *Escherichia coli*. *Microbiol Rev* **48:** 60–93

Walsh C (2003) Where will new antibiotics come from? *Nat Rev Microbiol* **1:** 65–70

Wang JC (1996) DNA topoisomerases. *Annu Rev Biochem* **65:** 635–692

Wanner BL (1983) Overlapping and separate controls on the phosphate regulon in *Escherichia coli* K12. *J Mol Biol* **166:** 283–308

Whitlock MC (2005) Combining probability from independent tests: the weighted *Z*-method is superior to Fisher's approach. *J Evol Biol* **18:** 1368–1373

Willmott CJ, Critchlow SE, Eperon IC, Maxwell A (1994) The complex of DNA gyrase and quinolone drugs with DNA forms a barrier to transcription by RNA polymerase. *J Mol Biol* **242:** 351–363

Witkin EM (1976) Ultraviolet mutagenesis and inducible DNA repair in *Escherichia coli*. *Bacteriol Rev* **40:** 869–907

Yang WC, Yanasugondha D, Webb JL (1958) The inhibition of mitochondrial respiration by 1,10-phenanthroline and 2,2′-bipyridine and the possible relationship to oxidative phosphorylation. *J Biol Chem* **232:** 659–668

Zamzami N, Marchetti P, Castedo M, Decaudin D, Macho A, Hirsch T, Susin SA, Petit PX, Mignotte B, Kroemer G (1995) Sequential reduction of mitochondrial transmembrane potential and generation of reactive oxygen species in early programmed cell death. *J Exp Med* **182:** 367–377

Zheng L, Cash VL, Flint DH, Dean DR (1998) Assembly of iron–sulfur clusters. Identification of an iscSUA–hscBA–fdx gene cluster from *Azotobacter vinelandii*. *J Biol Chem* **273:** 13264–13272

Published online: March 13, 2007